# Electrochemical Analysis of the Effect of Cr Coating the LiV$_3$O$_8$ Cathode in a Lithium Ion Battery with a Lithium Powder Anode

Jae Ha Lee, Jun Kyu Lee, and Woo Young Yoon*

Division of Materials Science and Engineering, Korea University, 5-ga, Anam-dong, Sungbuk-gu, Seoul 136-701, Republic of Korea

ABSTRACT: Rechargeable 2032-coin-type cells were produced with Li-powder anodes (i.e., Li-powder electrodes, LPEs) and either Cr-coated lithium trivanadate (Li$_{1+x}$V$_3$O$_8$, LVO) cathodes or uncoated LVO cathodes. The initial discharge capacity of a cell with an LPE and a Cr-coated LVO cathode (Cell$_{coated}$) was 252 mAh g^{-1} at a 0.2 C-rate and that of a cell with an LPE and an uncoated LVO cathode (Cell$_{bare}$) was 223 mAh g^{-1}. After the 50th cycle, Cell$_{coated}$ exhibited higher capacity retention (about 89%) than Cell$_{bare}$ (about 78%). Changes in the surface morphology of the Cr-coated LVO cathode were observed using scanning electron microscopy and energy-dispersive X-ray spectroscopy. The change in the electrical conductivity of the cell was measured using the impedance analysis. The electrochemical properties of the cells were also evaluated based on the differential capacity curve, voltage profiles, and capacity versus number of cycles.

KEYWORDS: lithium trivanadate, chromium coating, coating effect, lithium metal powder, lithium ion battery
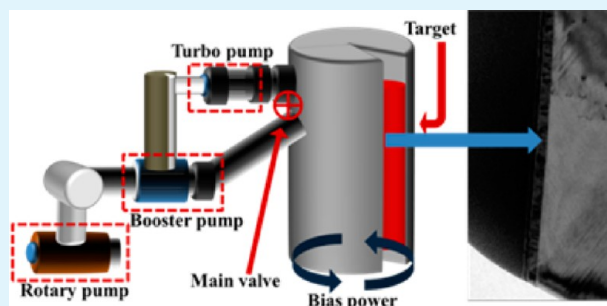
1. INTRODUCTION

Lithium metal has a high theoretical energy density (3860 mAh g^{-1}), which makes it a good anode material for use in secondary Li batteries. However, using Li metal in secondary batteries also has some disadvantages; for example, it cannot be used directly as an anode material in secondary batteries because of dendrite growth on the electrode surface during Li deposition.[1−5] Dendrite growth causes safety problems, cycle fading, and decreased cycling efficiency of secondary Li batteries. In our previous studies, we developed a compacted Li-powder electrode (LPE) that suppressed dendrite growth. Moreover, cycling efficiency and cycle fading were improved using an LPE.[6,7] The present research used Li powder for an anode material, instead of Li foil owing to its stability. The details of the characteristics of the Li-powder anode and its comparison with Li-foil anode have been reported elsewhere.[6−10] When Li metal is used directly as a battery anode, the nonlithiated cathodes must allow Li ions to be readily inserted and removed.

Recent studies show that vanadium pentoxide (V$_2$O$_5$), lithium trivanadate (Li$_{1+x}$V$_3$O$_8$, LVO), and their derivatives are promising cathode materials for Li secondary batteries.[11−14] LVO is a nonlithiated cathode material in which Li ions can readily intercalate into and deintercalate from the LVO's layered structure. Moreover, its theoretical capacity is above 280 mAh g^{-1}, and it has good cycle stability.[15−21] However, because of the low electrical and ion conductivities of LVO, cells produced with LVO electrodes exhibit capacity degradation and poor rate retention.[22−24] Moreover, researchers have recently investigated crack formation[25] and nonhomogeneous vanadium dissolution[26] in LVO electrodes, both of which have been found to cause capacity fading in LVO-based cells.

Although many research studies on doping of transition metals have been conducted to overcome these drawbacks, doping also has side effects that make the process difficult and cause eventual reduction of the vanadium ratio.[15−17] Chromium, a well-known conductive material, has been coated onto the LVO surface to improve its conductivity and prevent damage to the LVO cathode electrode during cycling. The present work reports the fabrication of a Cr-coated LVO cathode and the electrochemical properties of secondary cells produced with LPEs and LVO electrodes. The capacity and cycle stability of cells produced with bare and Cr-coated LVO cathodes are investigated. An explanation for the electrochemical effect of Cr coating is offered based on the finding that a direct coating on the electrode resolved the LVO processing issues without reducing the vanadium ratio.

2. EXPERIMENTAL SECTION

2.1. Preparation of Li-Powder Anode (Li-Powder Electrode, LPE). Li-powder particles were synthesized by the droplet emulsion technique (DET) illustrated in Figure 1a. Details of the technique have been previously discussed in the literature.[27,28] The droplets were spherical and had a diameter of about 7−10 μm (Figure 1b). The compacted Li-powder electrode was prepared using a stainless-steel-mesh (SUS) collector and a press, as shown schematically in Figure 2a. Figure 2b shows a scanning electron microscopy (SEM) image of the Li-powder particles contained in the compacted LPE.
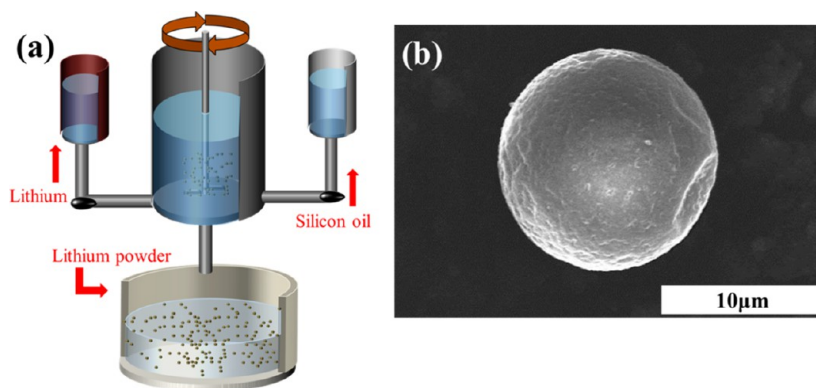
Figure 1. (a) Schematic of droplet emulsion technique (DET). (b) Scanning electron microscopy (SEM) image of a Li-powder particle produced using DET.
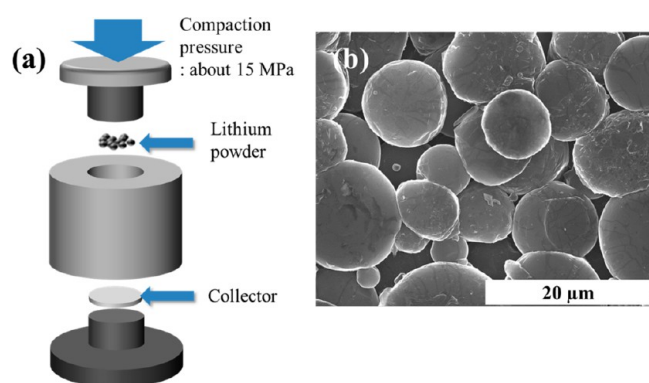

Figure 2. (a) Schematic of pressing apparatus used for producing Li-powder electrode (LPE). (b) SEM image of Li-powder particles that constitute a compacted LPE.

Although the LPE exhibited many pores, the Li-powder particles retained their original spherical shape.

2.2. Preparation of Cr-Coated LVO Electrode. The active materials of the bare LVO cathode were prepared from a deionized (DI) water slurry containing 80 wt % bare LVO (lath-shaped; GfE, Germany), 15 wt % acetylene black as the conductive material, and 5 wt % carboxymethyl cellulose (CMC) as the binder. The electrode was fabricated by casting the slurry onto aluminum foil, using water as the solvent.[29] Cr was coated onto the electrode by ion-beam sputtering (Dongwoo Surface Tech Co., Ltd., Republic of Korea) at 100 °C for 5 min. The process and experimental apparatus of sputtering were reported in detail elsewhere.[30] The surface of the deposited Cr layer was examined using SEM and energy-dispersive X-ray (EDX) spectroscopy.

2.3. Cell Assembly and Measurements. The surface morphologies of the bare and Cr-coated LVO electrodes were analyzed using a scanning electron microscope (Hitachi S-4300, Japan) equipped with an EDX analyzer. The alternating current (AC) impedance of the cells was measured in a Solartron SI1280B unit at frequencies ranging from 10^{-2} to 10^{5} Hz and with a 5-mV AC amplitude. The impedance data were then processed by the ZView software (Scribner Associates Inc., Southern Pines, NC, USA) and fitted to an electrical equivalent circuit. Electrochemical testing was galvanostatically performed using a WBCS 3000 instrument (WonAtech Inc., Republic of Korea) at a 0.2 C-rate with a cutoff voltage in the range 1.5−4.0 V. Electrochemical characterizations were performed using coin cells (CR2032) that were assembled in an Ar-filled glovebox.

Lithium phosphate hexafluoride ($LiPF_6$) (1 M, Techno Semichem Co, Republic of Korea) was dissolved in a mixture of ethylene carbonate (EC) and dimethyl carbonate (DMC) in a 1:1:1 volumetric ratio, and ethyl methyl carbonate (EMC) was used as an electrolyte.

3. RESULTS AND DISCUSSION

3.1. Characterization of Cr-Coated LVO Electrode. Figure 3 shows the XRD data of the bare LVO electrode and
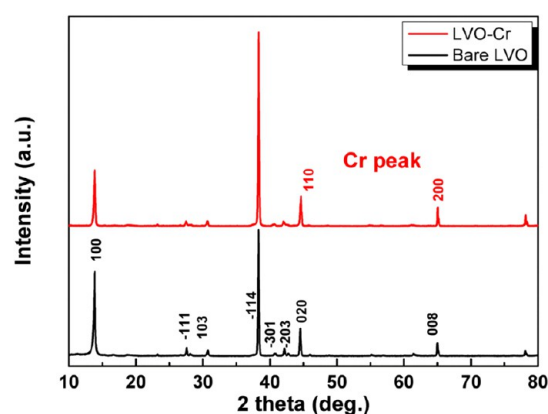

Figure 3. X-ray diffraction (XRD) patterns of LiV_3O_8 and Cr-coated LiV_3O_8 electrodes.

Cr-coated LVO electrode. The XRD patterns of the prepared LVO cells were collected between $2\theta = 10°$ and $80°$ at $2°$ min^{-1}. Because Al foil was used as the current collector, the Al peak appeared at 38.47° and 44.74° (JCPDS card no. 04-0787), with the peak at 38.47° being very strong in particular.[15−19] According to the JCPDS card no. 72-1193 for LiV_3O_8, all the observed diffraction peaks could be indexed to the pure monoclinic structure of space group $p21/m$, with unit cell parameters of $a = 6.680$, $b = 3.596$, and $c = 12.024$ Å, which was in agreement with the layered LiV_3O_8 structure.[25,31] The 14° peak was assigned to diffraction on the (100) plane, which was indicative of a layered structure. The absence of diffraction patterns of Cr might be a result of its low content.[31] Cr peaks were also observed at 44.39° and 64.57°, which were similar to the locations of the peaks of LiV_3O_8 and Al. The SEM images showed that the surface morphology of the bare LVO electrode (Figure 4a) consisted of sharp-edged lathlike structures. The average particle size of the LiV_3O_8 powder was 5 μm. The Cr-
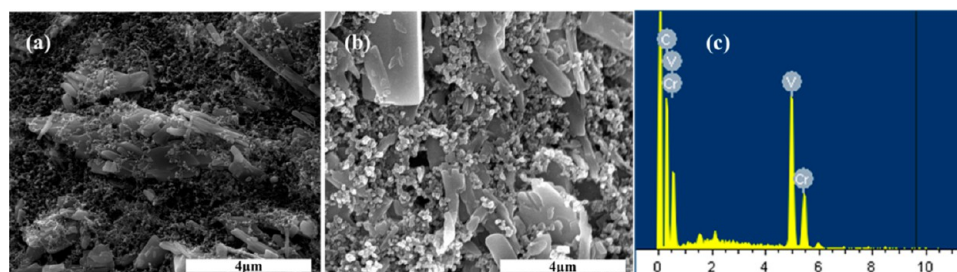
Figure 4. SEM images of surfaces of (a) bare and (b) Cr-coated lithium trivanadate (LVO) electrodes. (c) Energy-dispersive X-ray (EDX) spectroscopy pattern for Cr-coated LVO electrode.

coated electrode retained the lathlike structured surface morphology of the bare LVO electrode, as shown in Figure 4b. Cr, C (from the conductive material), and V were identified in the coated anode from the EDX spectroscopy (Figure 4c). The structure of the Cr-coated LVO electrode can be confirmed by the TEM image shown in Figure 5. The Cr
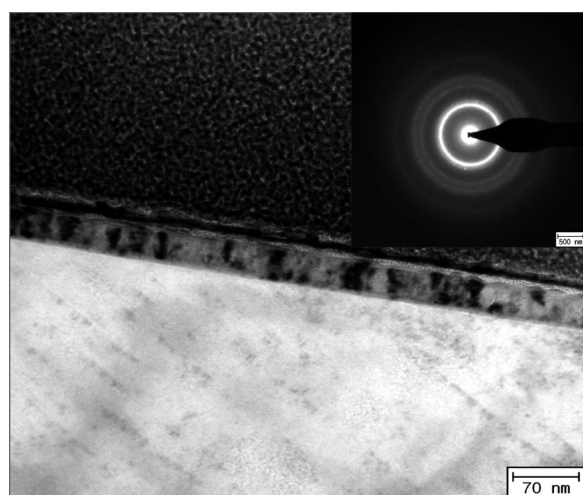

Figure 5. Transmission electron microscopy (TEM) image of Cr-coated LVO electrode. (inset) Selected area electron diffraction pattern.

coating was thin (about 50 nm) and could not block the Li site during charge/discharge. The selected area electron diffraction (SAED) patterns (see example in inset of Figure 5) of the Cr-coating layer indicated that it was polycrystalline. Figure 6a shows the surface of the Cr-coated LVO electrode and the result of electron probe microanalysis (EPMA) along the side-facet (Figure 6b), which clearly showed that Cr was uniformly coated on the electrode.

Figures 7a and b show the SEM images of the surfaces of the bare and Cr-coated LVO electrodes after 50 cycles, respectively; Figures 7c and d show the EDX spectra for both electrodes after 50 cycles. The SEM image of the bare LVO electrode (Figure 7a) revealed cracks on the surface of the active materials, but that of the Cr-coated LVO electrode (Figure 7b) showed that the initial electrode surface morphology remained relatively unchanged. The EDX spectrum for the bare LVO electrode after 50 cycles showed that F existed on the electrode (Figure 7c). Although the production of F on a cycled crystalline LVO electrode has never been reported previously, this result suggested that a reaction occurred between the electrode and the electrolyte and could reduce the capacity of the bare LVO electrode. The Cr coating

appeared to suppress the formation of reaction products on the surface of the Cr-coated LVO electrode. Tables 1 and 2 list the complete results of the EDX analysis for the bare and Cr-coated LVO electrodes, respectively. Fluorine was detected on the bare LVO electrode (Table 1), while it was not identified on the Cr-coated LVO electrode (Table 2). The active material of LVO dissolved in the LiPF6 electrolyte;[32] consequently, F was detected in the LVO cathode after cycling. However, because the Cr-coating suppressed the reaction between the electrolyte and the electrode, there was no F peak in the EDX spectrum after cycling, which highlights one of the major advantages of the Cr coating. On the basis of the XRD, SEM, TEM, and EPMA results, it could be confirmed that Cr only covered the surface of LiV_3O_8 and did not modify its layered structure.

3.2. Impedance Analysis of Cells with LPE/Bare LVO Electrodes and LPE/Cr-Coated LVO Electrodes. Figure 8a shows the impedance results for the cells with LPE/bare and LPE/Cr-coated LVO electrodes (referred to as $Cell_{bare}$ and $Cell_{coated}$, respectively). Figure 8b shows the equivalent circuit, and Table 3 lists the results of impedance data fitting. Basically, the Randles circuit structure was used for examining the electrochemical reaction on the electrode surface. In this equivalent circuit, R_s represents the sum of the ohmic resistances of the electrode and electrolyte. R_{ct} and C_{dl} are the charge transfer resistance and double-layer capacitance, respectively, in the parallel combination of the Randles circuit. The constant phase element (CPE) connected to R_{ct} in series induced a depressed semicircle in the corresponding Nyquist plot.[33−36] The parallel combination of R_{sei} and C_{sei} is associated with the resistance and capacitance on the electrode surface.[36−39] As shown in Figure 8a, the values of R_s, R_{sei}, and C_{sei} of the Cr-coated LVO electrode surface increased slightly owing to the Cr coating. However, the variations in R_{ct} suggested that $Cell_{coated}$ had a lower R_{ct} than $Cell_{bare}$ because of the absence of the reaction product on the electrode as the reaction was inhibited by the coating. Therefore, $Cell_{coated}$ had a higher conductivity than $Cell_{bare}$, an indication of its stable cycle characteristic. As the resistance decreased, the capacity was also increased. The impedance after 10 cycles showed remarkable changes as well. $Cell_{coated}$ showed stable cycle behavior and improved electrical conductivity because its R_{ct} was lower than that of $Cell_{bare}$.

3.3. Electrochemical behavior of Cells with LPE/Bare LVO Electrodes and LPE/Cr-Coated LVO Electrodes. Cycling tests were performed on cells with the compacted LPE as the anode. Figure 9 shows the voltage profiles for the charge and discharge capacities of $Cell_{bare}$ and $Cell_{coated}$. Both cells exhibited irreversible capacity after the initial cycle. The discharge capacity of $Cell_{coated}$ (252 mAh g^{-1}) was higher than that of $Cell_{bare}$ (223 mAh g^{-1}) by 11% at a 0.2 C-rate. Figure 10
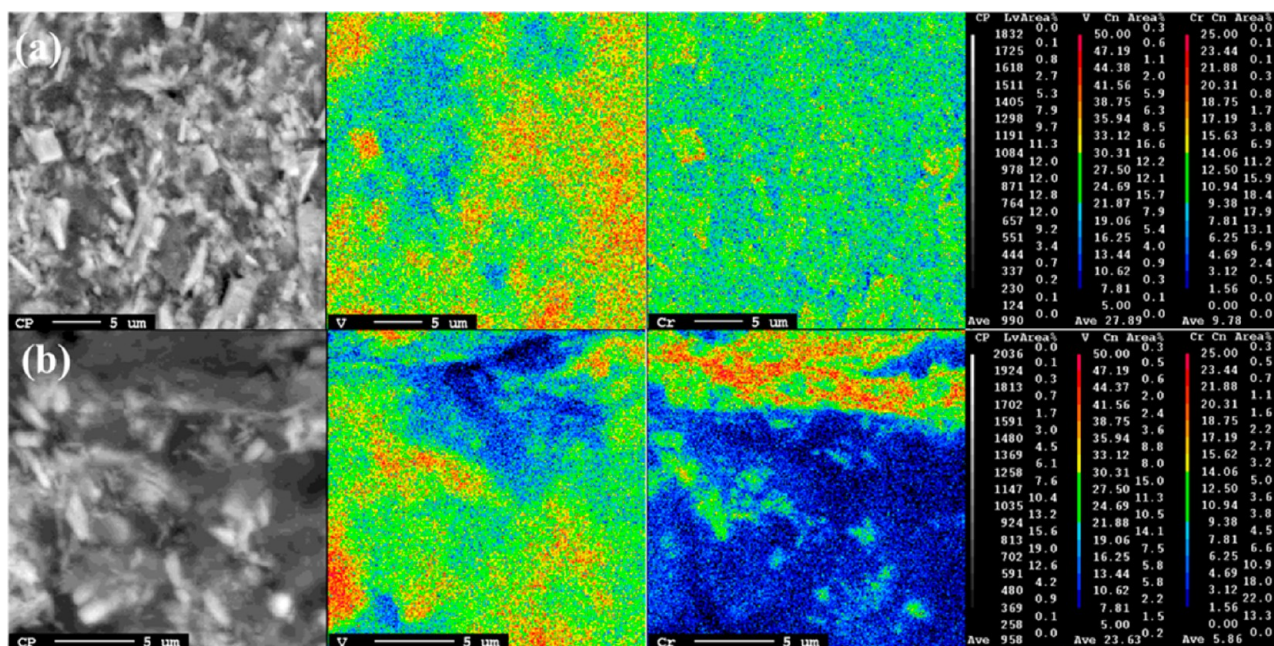
Figure 6. Electron probe microanalysis (EPMA) images of (a) Cr-coated LVO electrode surface and (b) side facet of Cr-coated LVO electrode.
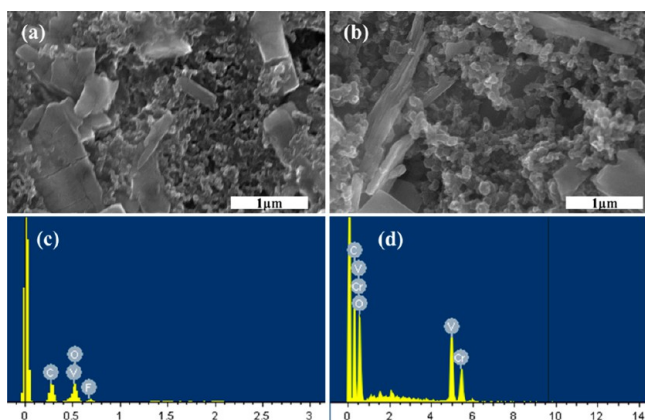

Figure 7. SEM images of (a) bare and (b) Cr-coated LVO electrode surface after 50 cycles. EDX spectroscopy pattern for (c) bare and (d) Cr-coated LVO electrodes measured after 50 cycles.

Table 1. Results of Energy-Dispersive X-ray (EDX) Spectroscopy Analysis of Bare Lithium Trivanadate (LVO) Electrode Measured after the 50th Cycle

element	weight %	atomic %
C	28.72	41.35
O	37.74	40.80
F	11.33	10.32
V	22.21	7.54
total	100.00	

shows the results of the cycling test. The discharge capacity profiles for both cells were obtained during 50 cycles at a 0.2 C-rate and a cutoff in the range 1.5−4.0 V (versus Li/Li$^+$). The Cr coating significantly improved the discharge capacity of Cell$_{coated}$ because of the high electrical conductivity of Cr. Figure 10 also shows that the initial discharge capacity of Cell$_{coated}$ was 252 mAh g^{-1}, which decreased to 226 mAh g^{-1} after 50 cycles. Cell$_{bare}$ had an initial discharge capacity of 223 mAh g^{-1}, which decreased to 175 mAh g^{-1} after 50 cycles. The

Table 2. Results of EDX Analysis of Cr-Coated LVO Electrode Measured after 50th Cycle

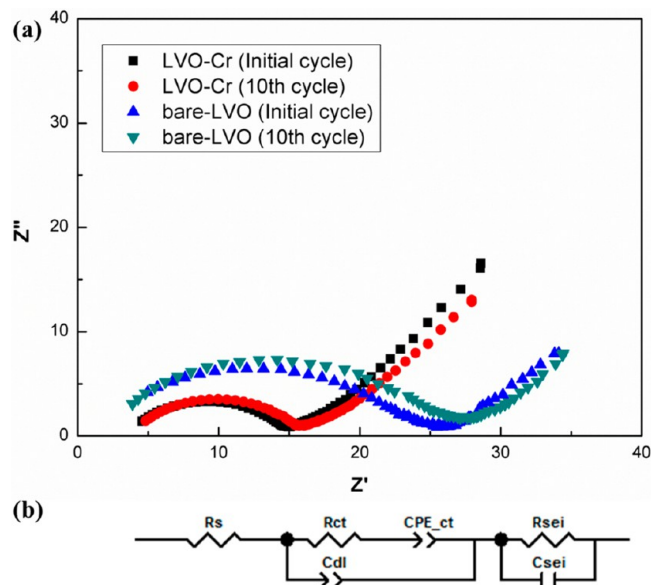| element	weight %	atomic %
C	32.01	50.28
O	30.46	35.92
V	24.97	9.25
Cr	12.56	4.56
total	100.00	

Figure 8. (a) Impedance analysis of cells produced with LPE/bare and LPE/Cr-coated LVO electrodes. (b) Impedance values obtained on the basis of equivalent circuit.

capacity retention of Cell$_{coated}$ was 89%, which was much higher than 78% shown by Cell$_{bare}$. As the Cr coating on the electrode had a thickness of only ~50 nm, the actual weight change before and after the application of coating was below 0.05%.

Table 3. Results of Impedance Fitting Data

|	bare LVO (before cycle)	bare LVO (after 10th cycle)	Cr-coated LVO (before cycle)	Cr-coated LVO (after 10th cycle)
R_s (Ω/cm^2)	1.52	1.28	2.656	2.598
R_{ct} (Ω/cm^2)	18.12	22.52	4.049	4.256
$CPE\_ct - T(\mu F)$	0.11874	0.12113	0.65389	0.66078
$CPE\_ct - P$	0.10083	0.099898	0.44977	0.46573
$C_{dl} - T(\mu F)$	0.00003708	0.00002718	0.00021339	0.00021103
$C_{dl} - P$	0.7066	0.7221	0.68143	0.6796
R_{sei} (Ω/cm^2)	13.67	15.62	14.6	20.38
C_{sei} (μF)	1.926	2.084	3.589	4.007
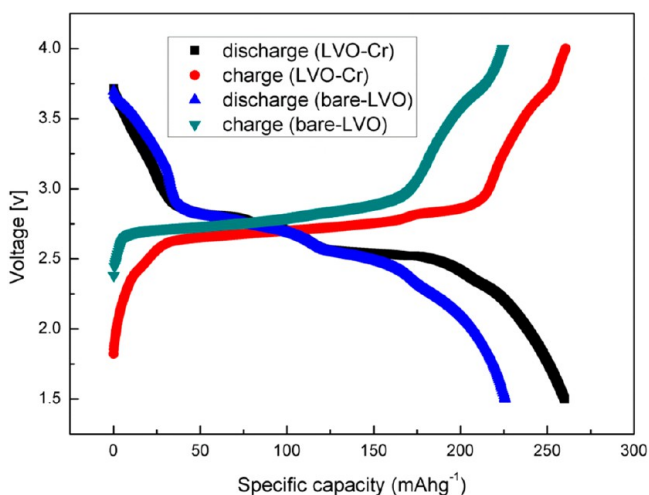
Figure 9. Voltage profiles measured during the initial cycle for cells produced with LPE/bare and LPE/Cr-coated LVO electrodes.
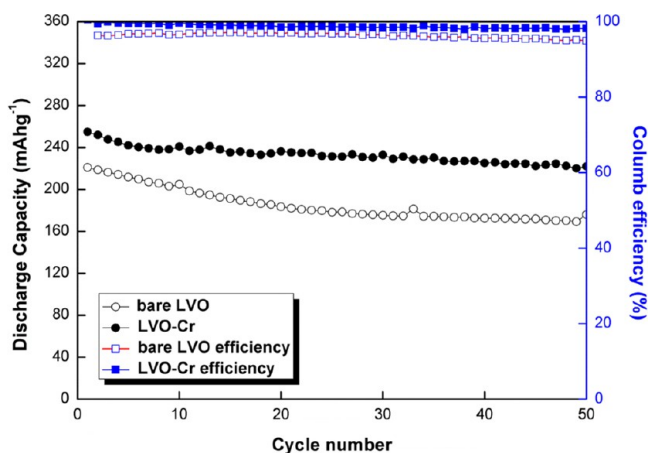

Figure 10. Discharge capacity profiles for cells produced with LPE/bare and LPE/Cr-coated LVO electrodes.

This change had little effect on the calculation of the capacity. Moreover, when the Cr-coated LVO cell with a higher amount of Cr was tested to investigate the effect of coating thickness, the highly coated cell (over ~100 nm thick) showed poor cycle capacity. Although Cr's high electrical conductivity and the protection it offered the electrode from reaction with the electrolyte enhanced the LVO's electrochemical properties, an optimal thickness appeared to exist. Figure 11 shows a comparison of the cyclic performance of both cells at 0.2−2 C-rate. The discharge capacity decreased as the C-rate increased, and the specific capacities of the Cell$_{coated}$ were 248 mAh g^{-1} at 0.2 C-rate, 221 mAh g^{-1} at 0.5 C-rate, 180 mAh g^{-1}
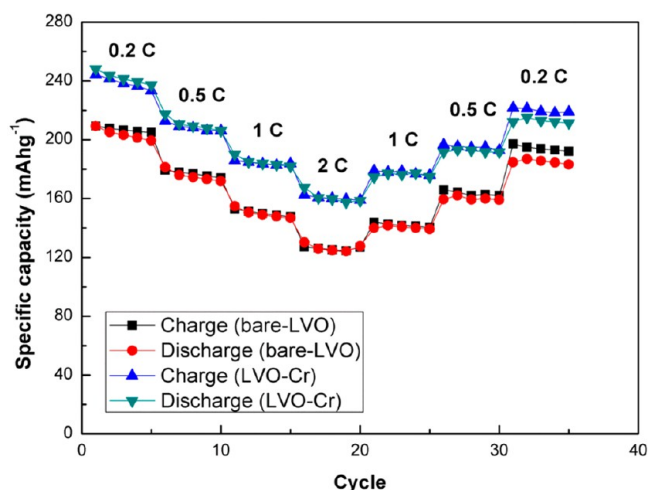

Figure 11. Rate capacity comparison of LPE/bare LVO and LPE/Cr-coated LVO electrodes.

at 1 C-rate, and 158 mAh g^{-1} at 2 C-rate. Upon cycling back to 0.2 C-rate, Cell$_{coated}$ delivered a capacity of 231 mAh g^{-1}. These results implied that the performance of Cell$_{coated}$ was much better than Cell$_{bare}$ in every C-rate section.

The above results suggest that the capacity retention of a cell can be further increased by adding a Cr-coated LVO cathode because the Cr coating suppresses the formation of reaction products on the electrode surface while maintaining the surface morphology of the LVO electrode. Figure 12 shows the differential capacity plots of Cell$_{bare}$ and Cell$_{coated}$ measured during the 10th, 20th, and 30th cycles. The anodic peaks for Li ion insertion into the LVO appeared at 2.6−2.8 V while the cathodic peaks appeared at 2.7−2.8 V. The differential capacity plot for Cell$_{bare}$ in each measured cycle exhibited peaks associated with an unstable chemical reaction, while that for Cell$_{coated}$ exhibited peaks associated with a stable chemical reaction. This result indicated that the Cr coating on a cell's electrode improved the electrochemical properties. In each cycle, Cell$_{coated}$ showed a higher peak intensity than Cell$_{bare}$, proving that the Cr coating assisted in attaining higher insertion capacity and faster kinetics.[25]

4. CONCLUSIONS

Li-powder particles were synthesized using the droplet emulsion technique and were used directly as an anode material. Cr was coated onto an LVO-cathode electrode by sputtering. The EDX spectrum and the results of EPMA indicated that the Cr coating on the electrode surface was uniform. The results of the impedance analysis showed that the cell produced with the LPE and Cr-coated LVO cathode had a lower charge-transfer resistance than that produced with the
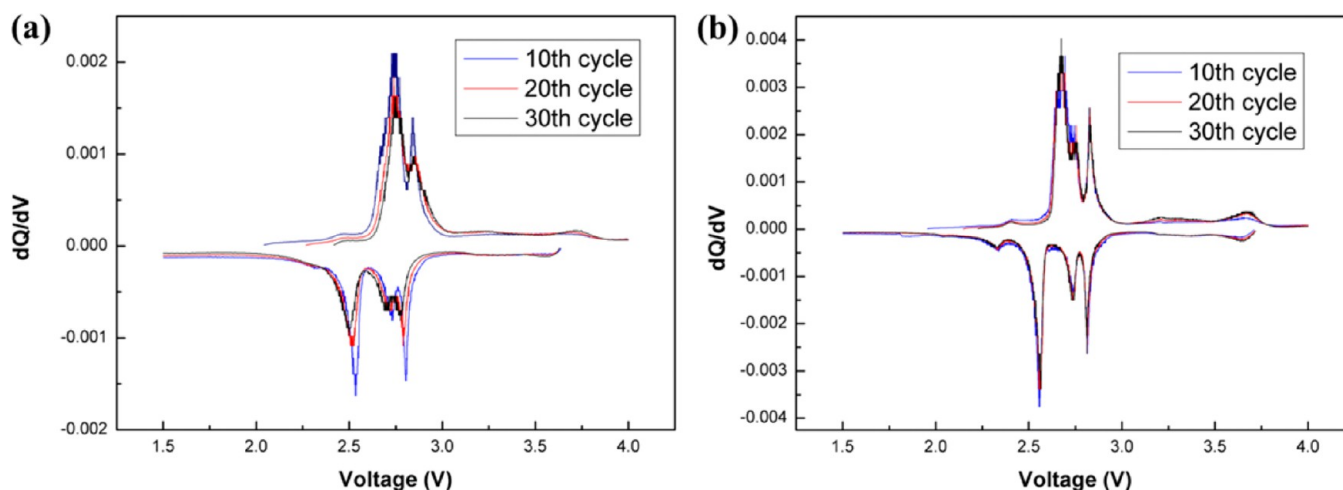
Figure 12. Differential capacity plots of (a) Cell$_{bare}$ and (b) Cell$_{coated}$ measured during the 10th, 20th, and 30th cycles.

LPE and bare LVO cathode, indicating that the capacity of the first cell was increased owing to the high electrical conductivity of the Cr-coated LVO cathode. The same cell exhibited an initial discharge capacity of 252 mAh g^{-1} at a 0.2 C-rate, which was higher than the capacity (223 mAh g^{-1}) of the cell produced with the LPE and bare LVO cathode. After the 50th cycle, the cell produced with the LPE and Cr-coated LVO cathode had a higher capacity retention (about 89%) than the cell produced with the LPE and bare LVO cathode (about 78%). The EDX spectra for the cycled LVO electrodes indicated the presence of fluorine on the surface of the uncoated LVO electrode but not on the surface of the Cr-coated LVO electrode. This result suggested that the Cr coating prevented the reaction between the electrolyte and the electrode, and in turn, the cycling efficiency of the cell produced with the Cr-coated LVO electrode was increased. Therefore, the Cr coating not only increased the electrical conductivity of the LVO electrode but also acted as a sound interface layer, protecting the LVO electrode against further reaction with the electrolyte.

AUTHOR INFORMATION

Corresponding Author
*E-mail: wyyoon@korea.ac.kr.

Present Address
Department of Materials Science and Engineering, Korea University, 5Ga, Anam-dong, Sungbuk-Gu, Seoul 136-701, Republic of Korea.

Author Contributions
The manuscript was written through contributions of all authors. All authors have given approval to the final version of the manuscript.

Notes
The authors declare no competing financial interest.

ABBREVIATIONS

AC, alternating current
CMC, carboxymethyl cellulose
DET, droplet emulsion technique
DI, deionized (water)
DMC, dimethyl carbonate
EC, ethylene carbonate
EDX, energy-dispersive X-ray (spectroscopy)
EMC, ethyl methyl carbonate
EPMA, electron probe microanalysis
LPE, Li-powder electrode
LVO, lithium trivanadate
SEM, scanning electron microscopy
SUS, stainless-steel mesh
XRD, X-ray diffraction

REFERENCES

(1) Mori, M.; Naruoka, Y.; Naoi, K.; Fauteux, D. *J. Electrochem. Soc.* **1998**, *145*, 2340−2348.
(2) Aurbach, D.; Zinigard, E.; Cohen, Y.; Teller, H. *Solid State Ionics* **2002**, *148*, 405−416.
(3) Seong, I. W.; Hong, C. H.; Kim, B. K.; Yoon, W. Y. *J. Power Sources* **2008**, *178*, 769−773.
(4) Yamaki, J. I.; Tobishima, S. I.; Sakaurai, Y.; Saito, K. I.; Hayashi, K. *J. Appl. Electrochem.* **1998**, *28*, 135−140.
(5) Li, J.; Xiong, S.; Liu, Y.; Ju, Z.; Qian, Y. *ACS Appl. Mater. Interfaces* **2013**, *5*, 981−988.
(6) Kim, J. S.; Yoon, W. Y. *Electrochim. Acta* **2004**, *50*, 531−534.
(7) Kim, J. S.; Yoon, W. Y.; Yi, K. Y.; Kim, B. K.; Cho, B. W. *J. Power Sources* **2007**, *165*, 620−624.
(8) Kim, J. S.; Kim, B. K; Yoon, W. Y. *J. Power Sources* **2006**, *163*, 258−263.
(9) Kim, W. S; Yoon, W. Y. *Electrochim. Acta* **2004**, *50*, 541−545.
(10) Hong, S. T.; Kim, J. S.; Lim, S. J.; Yoon, W. Y. *Electrochim. Acta* **2004**, *50*, 535−539.
(11) Fu, L. J.; Liu, H.; Li, C.; Wu, Y. P.; Rahm, E.; Holze, R.; Wu, H. Q. *Prog. Mater. Sci.* **2005**, *50*, 881−928.
(12) Liu, J.; Xia, H.; Xue, D.; Lu, L. *J. Am. Chem. Soc.* **2009**, *131*, 12086−12087.
(13) Liu, J.; Zhou, Y.; Wang, J.; Pan, Y.; Xue, D. *Chem. Commun.* **2011**, *47*, 10380−10382.
(14) Liu, J.; Liu, W.; Wan, Y.; Ji, S.; Wang, J.; Zhou, Y. *RSC Adv.* **2012**, *2*, 10470−10474.

7063

dx.doi.org/10.1021/am401334b | *ACS Appl. Mater. Interfaces* 2013, 5, 7058−7064

(15) Feng, Y.; Li, Y.; Hou, F. *Mater. Lett.* **2009**, *63*, 1338−1340.

(16) Y. Liu, F.; Zhou, X.; Guo, Y. *Electrochim. Acta* **2009**, *54*, 3184−3190.

(17) Feng, C. Q.; Huang, L. F.; Guo, Z. P.; Wang, J. Z.; Liu, H. K. *J. Power Sources* **2007**, *174*, 548−551.

(18) Zhao, M.; Jiao, L.; Yuan, H.; Feng, Y.; Zhang, M. *Solid State Ionics* **2007**, *178*, 387−391.

(19) Kumagai, N.; Yu, A. *J. Appl. Electrochem.* **1997**, *27*, 953−958.

(20) Wang, G. J.; Fu, L. J.; Wang, B.; Zhao, N. H.; Wu, Y. P.; Holze, R. *J. Appl. Electrochem.* **2008**, *38*, 579−581.

(21) Xu, X.; Luo, Y.; Mai, L.; Zhao, Y.; An, Q.; Xu, L.; Hu, F.; Zhang, L.; Zhang, Q. *NPG Asia Mater.* **2012**, *4*, e20.

(22) Jiao, L.; Li, H.; Yuan, H.; Wang, Y. *Mater. Lett.* **2008**, *62*, 3937−3939.

(23) Panero, S.; Pasquali, M.; Pistoia, G. *J. Electrochem. Soc.* **1983**, *130*, 1225−1227.

(24) Nassau, K.; Murphy, D. W. *J. Non-Cryst. Solids* **1981**, *44*, 297−304.

(25) Chew, S. Y.; Feng, C.; Ng, S. H.; Wang, J.; Guo, Z.; Liu, H. *J. Electrochem. Soc.* **2007**, *154* (7), A633−A637.

(26) Fergus, J. W. *J. Power Sources* **2010**, *195*, 939−954.

(27) Park, M. S.; Yoon, W. Y. *J. Power Sources* **2003**, *114*, 237−243.

(28) Yoon, W. Y.; Paik, J. S.; LaCourt, D.; Perepezko, J. H. *J. Appl. Phys.* **1986**, *60*, 3489−3494.

(29) Seong, I. W.; Kim, K. T.; Yoon, W. Y. *J. Power Sources* **2009**, *189*, 511−514.

(30) Lee, J. K.; Kim, B. K.; Yoon, W. Y. *J. Electrochem. Soc.* **2012**, *159* (11), A1844−A1848.

(31) Cao, X. Y.; Guo, L. J.; Liu, J. P.; Xie, L. L. *Int. J. Electrochem. Sc.* **2011**, *6*, 270−278.

(32) Gao, X.; Wang, J.; Chou, S.; Liu, H. *J. Power Sources* **2012**, *220*, 47−53.

(33) Shiraishi, S.; Kanamura, K.; Takehara, Z. *J. Electrochem. Soc.* **1999**, *146*, 1633−1639.

(34) Jamnik, J.; Maier, J. *Phys. Chem. Chem. Phys.* **2003**, *5*, 5215−5220.

(35) Sinha, N. N.; Munichandraiah, N. *ACS Appl. Mater. Interfaces* **2009**, *1* (6), 1241−1249.

(36) Xiao, P.; Zhang, Y.; Garcia, B. B.; Sepehri, S.; Liu, D.; Cao, G. *J. Nanosci. Nanotechno.* **2008**, *8*, 1−11.

(37) Qian, X.; Gu, N.; Cheng, Z.; Yang, X.; Wang, E.; Dong, S. *Electrochim. Acta* **2001**, *46*, 1829−1836.

(38) Lee, K. H.; Song, S. W. *ACS Appl. Mater. Interfaces* **2011**, *3*, 3697−3703.

(39) Rao, C. V.; Reddy, A. L. M.; Ishikawa, Y.; Ajayan, P. M. *ACS Appl. Mater. Interfaces* **2011**, *3*, 2966−2972.